

NASA TM X-65895

# ELECTRIC FIELDS IN THE MAGNETOSPHERE

J. P. HEPPNER

MAY 1972

FACILITY FORM 602

N72-25829  
(ACCESSION NUMBER)

\_\_\_\_\_ (THRU)

20  
(PAGES)

G3  
(CODE)

NASA-TM-X-65895  
(NASA CR OR TMX OR AD NUMBER)

30  
(CATEGORY)



**GODDARD SPACE FLIGHT CENTER**  
**GREENBELT, MARYLAND**

Reproduced by  
**NATIONAL TECHNICAL  
INFORMATION SERVICE**  
U S Department of Commerce  
Springfield VA 22151



ELECTRIC FIELDS IN THE MAGNETOSPHERE

J. P. Heppner  
NASA Goddard Space Flight Center  
Greenbelt, Md., U.S.A.

May 1972

For publication in the proceedings of the "Symposium on Critical Problems of Magnetosphere Physics," Madrid, May 1972

# ELECTRIC FIELDS IN THE MAGNETOSPHERE

J. P. Heppner  
NASA Goddard Space Flight Center  
Greenbelt, Md., U.S.A.

Abstract. Two techniques, tracking the motions of Ba<sup>+</sup> clouds and measuring the differences in floating potential between symmetric double probes, have been highly successful in: (a) demonstrating the basic convective nature of magnetospheric electric fields, (b) mapping the global patterns of convection at upper ionosphere levels, and (c) revealing the physics of electric currents in the ionosphere and the importance of magnetosphere-ionosphere feedback in altering the imposed convection. The basic pattern of anti-solar convection across the polar cap and night toward day convection in both the evening and morning sectors at auroral belt latitudes persists at all levels of activity. The dawn-dusk potential drop across the polar cap (anti-solar convection) ranges from 20 to 100 kilovolts with the most typical values in the center of this range. The sum of morning and evening (night toward day convection) potential drops in the adjacent auroral belts roughly equals the polar cap drop in the opposite sense as expected. It has been found that different types of detailed variations in the distribution of polar cap fields correlate closely with select directions of the interplanetary magnetic field. These correlations are not of a type that might be expected from past correlations with Kp and thus they may open the door for a better understanding of the transfer of momentum from the solar wind to the magnetosphere. Recent IMP-I measurements clearly show anti-solar convection in a narrow zone inside the magnetopause.

## INTRODUCTION

Prior to 1964 magnetospheric electric fields could only be inferred from interpretations of phenomena and indirect measurements: for example, (a) from model descriptions of the potentials and ionospheric conductivities that would give ionospheric electric currents compatible with observations of magnetic field variations, and (b) from optical observations of auroral motions and radar observations of the apparent motions of electron density irregularities with the assumption that these were convective motions. In 1964 the initial Ba<sup>+</sup> release experiments were conducted at low latitudes (Föppl et al., 1965) and the first proposal appeared for d.c. electric field measurements using the long symmetrical antenna, or double probe, floating potential technique (Aggson and Heppner, 1964). The era of direct measurement of magnetospheric electric fields was effectively entered in 1966-67 when the symmetric double probe technique was critically tested and both the probe and Ba<sup>+</sup> drift techniques were used in the upper ionosphere at auroral latitudes (Haerendel, et al., 1969; Aggson, 1969; Mozer and Bruston, 1967; Föppl, et al., 1968; Wescott, et al., 1969). In 1967 probe measurements were also initiated on satellites on OVI-10 but a failure in one of the two probes restricted results to the detection of convection boundaries and the study of field irregularities (Heppner, 1969; Maynard and Heppner, 1970).

Progress in the subsequent 5 years has been substantial. Results from the two techniques are comparable and complementary. The Ba<sup>+</sup> drift technique with multiple releases permits study of changes in the time-space distribution of  $E$  over select regions. The disadvantages are: (1) that measurements below altitudes of several thousand kilometers are seasonally restricted to the local times and latitudes of twilight, and (2) at large distances in weak magnetic fields the drifts become difficult to interpret as a consequence of destroying the ambient  $\beta$  (i.e., balance of plasma and magnetic field energy densities). The probe technique has the advantage of not being restricted in terms of time and latitude, or distance from the earth when the separation of the two elements of the double probe is adequately large. The relative disadvantage is that the vehicle motion does not permit studying the time history of  $E$  at a select location.

New indirect means of deducing magnetospheric fields have also been introduced: such as, observing the radial motions of whistler ducts (Carpenter and Stone, 1967, the use of double probes on balloons (Mozer and Serlin, 1969), and modelling the time-space history of plasmas encountered in synchronous orbit (McIlwain, 1971). As these measurements involve assumptions of comparable uncertainty to other indirect measurements, and because of restrictions on the length of this paper, only direct measurements will be discussed here.

Existing direct measurements of electric fields can be spatially categorized in terms of: (1) those taken below several thousand kilometers in altitude, and (2) measurements at great distances. Global distributions of  $\underline{E}$  as well as detailed relationships with ionospheric phenomena (e.g., electric currents, aurora, winds, etc.) are currently based on the low altitude measurements. Accurate d.c. measurements at great distances within the magnetosphere have only recently become available and presently relate primarily to select times and locations (e.g., the magnetopause). They have, however, also shown that the weak, and thus difficult to measure, magnitudes present through most of the magnetosphere are compatible with magnitudes expected from extrapolation of low altitude measurements along the magnetic field using the frozen-in field relationship  $\underline{E} + \underline{v} \times \underline{B} = 0$ . Thus in this presentation the low altitude measurements, taken near the focal point of the magnetic field lens, occupy most of the discussion. These measurements are presented where taken and are not extrapolated into outer magnetospheric regions simply because the author does not believe that existing magnetic models permit accurate field line tracing to great distances from high latitude regions. The reader is thus free to apply his own choice of field line models.

#### AURORAL BELT ELECTRIC FIELDS

It is convenient to define the "polar cap" as being the polar region of anti-solar convection and the "auroral belt" as being the adjacent lower latitude belt in which the convection is toward the sun roughly along parallels of latitude. These definitions, in addition to being convenient, are at least statistically accurate: simply from noting that the "auroral belt" or "auroral oval" defined in terms of visible aurora occurrences lies within the statistical boundaries of sunward convection. In addition to this statistical coincidence there are a number of examples from the convective motions of  $Ba^+$  clouds where the highest latitude visible aurora was either coincident with the latitudinal reversal from sunward convection to anti-solar convection or at a lower latitude than this transitional boundary. The possibility that aurora occasionally occurs also well within the "polar cap" (as defined) is not, however, ruled out and is perhaps to be expected if the term "polar cap aurora" used in the past by some observers has a meaning distinct from other aurora. The definitions above, do however appear to conflict with Frank and Gurnett's (1971) conclusion that auroral arcs are associated with anti-solar convection poleward from the reversal region as well as at the location of convective reversal. In general, following the definition here, one would expect most (e.g., at least 90%) auroral arcs to be located within, or at the boundary of, the belt of sunward convection.

Some of the earliest  $Ba^+$  release and sounding rocket probe experiments (referenced previously; also see Wescott, et al., 1970; Haerendel and Lust, 1970) produced several general results in addition to revealing magnitudes, gradients, irregularity structure, etc.; these were:

- (a) auroral electrojet currents producing surface magnetic disturbances were identified as Hall currents (i.e.,  $\underline{E} \perp \underline{B}$ ,  $\underline{E} \parallel \underline{AB}$ ,  $\underline{E} \perp \underline{i}$ ),
- (b) the convective pattern suggested by the assemblage of measurements was in agreement with models characterized as "two cell" models,
- (c) magnitudes,  $|\underline{E}|$ , decreased within magnetic shells where the ionospheric conductivity was apparently enhanced by auroral precipitation, and

- (d) magnitudes of  $\tilde{E}$  were not closely related to the magnitudes of the magnetic disturbance,  $\Delta\tilde{B}$ , and this indicated that the intensity of electrojet currents was more closely dependent on the conductivity than on  $|\underline{E}|$ .

Auroral Belt: Gross Characteristics. The generality of (b) and (d) above has been demonstrated well beyond evidence from additional rocket experiments in that these results are obviously apparent on a much larger scale from satellite measurements (Cauffman and Gurnett, 1971; Heppner, 1972a). Figure 1 shows the electric field observed on two polar passes of OGO-6 after subtraction of the  $\underline{V} \times \underline{B}$  fields from both the satellites motion and the earth's rotation. The satellite enters the auroral belt convection near 18<sup>h</sup> magnetic time and observes a "poleward" electric field. The field reverses to the dawn-dusk direction on entering the polar cap and remains relatively uniform in crossing to the dawn side where it again reverses on entering the auroral belt near 6<sup>h</sup>. Near 6<sup>h</sup> the plus direction is "equatorward." This general sequence of field directions for the dawn-dusk component is almost always present for traverses between mid-evening and mid-morning sectors intersecting the noon-midnight meridian roughly above 80° on the dayside and 75° on the nightside. Existence and average sign appears to be independent of magnetic activity conditions, stages of substorm enhancements, interplanetary field directions, etc. Multiple reversals are, however, observed on many passes within spatially isolated sub-regions of the general sequence and on more rare occasions the auroral belt-polar cap boundary may shift all the way to the pole, from either the dawn or dusk side, and thus greatly distort the latitudinal distribution of the usual sequence.

Field magnitudes, as opposed to directions, are much less predictable although there is a definite tendency for the integrated magnitude (i.e., the potential change) to increase with increasing levels of magnetic activity. Within the auroral belts there is also a statistical tendency for maximum field intensities to occur most frequently in the high latitude half of the belt. The changes in potential across the evening and morning auroral belts (e.g., near 18<sup>h</sup> and 6<sup>h</sup>, respectively) are frequently highly unequal (i.e., considerably more unbalanced than suggested by Figure 1) but the sum of the potential changes for the two auroral belts corresponds closely to the potential drop across the polar cap. The magnitude of this potential drop varies considerably for different traverses, roughly from near 20 kev to over 100 kev, with values in the center of this range (e.g., 40 to 70 kev) being most common under conditions of moderate magnetic variation, such as for Kp=3 (Heppner, 1972a).

Figure 2(b) illustrates the "two cell" convective flow in the near midnight region where the anti-solar polar cap convection has to split along east-west paths that continue the flow back toward the sun through both the morning and the evening hours. Although highly idealized here, this split is readily identified in terms of the Harang discontinuity (Heppner, 1972b) in electrojet currents (i.e., the dashed line shown crossing the 60° - 70° zone between 23<sup>h</sup> and 21<sup>h</sup>30<sup>m</sup> magnetic local time). Figure 2(c) indicates the range of variability in the magnetic local time location of the Harang discontinuity from past studies of auroral motions and magnetic disturbance patterns. Figure 2(b) is drawn compatible with the arrows shown on Figure 2(a). The Figure 2(a) solid arrows represent mean motions of Ba<sup>+</sup> clouds released on various dates in the vicinity of the Harang discontinuity in experiments conducted by the Goddard Space Flight Center. They are plotted relative to the instantaneous location of the discontinuity, as indicated by simultaneous magnetic and auroral observations, rather than at their true location in magnetic time and latitude; similarly the location of the discontinuity is arbitrarily fixed for the purpose of illustration (see Heppner, 1972b). Dotted arrows in Figure 2a represent typical mean motions at other locations of GSFC Ba<sup>+</sup> drift experiments; as they are remote from the discontinuity they are shown approximately at their true locations. The observations remote from the discontinuity, dotted arrows, are completely compatible with satellite probe measurements. Flow directions from Ba<sup>+</sup> releases of the Max Planck Institut (Haerendel, 1971) both near and remote from the Harang discontinuity appear to be consistent with Figure 2. Although convective patterns near and remote from the Harang discontinuity can be realistically

constructed from data, the data is not adequate to construct more comprehensive diagrams bridging the gap that exists poleward from the discontinuity. There is some evidence that eddy structures need to be included.

On the dayside, and particularly in the late morning hours, between  $70^\circ$  and  $85^\circ$  it is frequently not possible to make a distinction between auroral belt and polar cap fields either in terms of sign or field variability. Large fluctuations and frequent sign reversals are typical (Heppner, 1972a). Aggson and Bohse (1972) have, however, shown that a relative symmetric and simple two-cell configuration (similar to the general configuration drawn by Axford and Hines, 1961) appears on the dayside as well as the nightside when many traverses of OGO-6 are averaged.

Auroral Belt: Small Scale Characteristics. Early findings, (a) above, that the vector properties of  $\underline{E}$ ,  $\underline{B}$ , and  $\underline{AB}$  relative to the orientation of nearby auroral forms were consistent with attributing electrojet currents to the Hall conductivity have since been repeated on numerous occasions and are also consistent with observations on a broader scale from satellites. Interest has thus shifted to examining cases that have the appearance of contradicting this simple picture. These cases are found in space-time proximity to the Harang discontinuity and are usually associated with the dynamic changes accompanying auroral break-up. Thus, there is the obvious question as to whether or not any simple interpretation can be applied; for example, Wescott, et al. (1970) observed northward moving auroral forms crossing the paths of south and westward moving  $Ba^+$  clouds, and Haerendel (1971) has reported crossing paths for a case of a westward travelling surge. However, such cases represent contradictions only if one assumes that the auroral motions are purely convective motions. This assumption is not very plausible if the primary auroral particles have energies in excess of several kev--particularly if the simultaneous magnetospheric configuration is such that abnormal gradient and curvature drifts are likely and acceleration processes associated with the break-up phenomena are involved. Thus, these examples, do not provide a justification for explaining surface magnetic disturbances in terms of ionospheric Pedersen and Cowling currents.

Haerendel (1971) quotes six authors as recently suggesting that the meridional component of the electric field arises from polarization effects in the ionosphere under an assumption that the primary field is east-west, but concludes that data do not fit this type of model. It appears likely that in developing such models authors have generalized on the existence of westward electric fields in the vicinity of the Harang discontinuity where many rocket experiments are conducted relative to auroral activity. It should be apparent that westward fields in this region are exactly what is expected, and required, for convection continuity in the two-cell configuration.

Examples, noted above, where auroral forms have crossed the paths of drifting  $Ba^+$  clouds also illustrate the finding, (c) above, initially by Aggson (1969), that the magnitude of the electric field decreases within the shells of visible aurora. In addition to cases of actual path crossings there are a greater number of cases where crossings have not taken place but where  $Ba^+$  drift velocities have decreased as aurora moved close to a cloud. Assuming that the ionization in the fringe regions of an auroral form is enhanced relative to more remote areas these observations also suggest an anti-correlation between ionization and electric field intensity in terms of the local distribution of electric field intensities. An important related observation is that unlike numerous models which assume that strong polarization fields are created in the ionosphere, and particularly in the regions bordering aurora, the data do not reveal field enhancements in adjacent regions. In an auroral environment with large horizontal gradients in ionization density this means that filamentary field aligned currents must flow freely into and out of the ionosphere for local continuity of both the Hall and Pedersen currents. On a large scale the net flow from the filaments providing continuity for the Hall currents leads to a field aligned current system that offers an explanation for the horizontal magnetic disturbance observed in polar cap regions (Heppner et al., 1971)

As noted by Heppner et al. (1971) the anti-correlation between  $|\underline{E}|$  and lower ionosphere electron densities cannot, in general, be a linear relationship which in turn implies that the magnetosphere must act as a current generator as well as a voltage generator. This dual property, further complicated by the fact that ionospheric conductivities at the northern and southern hemisphere feet of a given flux tube will not in general be equal, makes the total problem of ionospheric feedback extremely complicated. It should perhaps be surprising that the anti-correlation has appeared consistently to date. Conditions which violate  $\underline{E} + \underline{v} \times \underline{B} = 0$  (e.g., large pressure gradients, Hines, 1964), or by any means destroy the continuity along field lines between the two hemispheres, could also affect the anti-correlation relationship. In terms ofOGO-6 observations of differences in the irregularity structure in the two hemispheres it appears that these conditions are more likely to be found in high latitude aurora than in aurora located in the central or lower latitude portions of the auroral belt convection.

The electric field parallel to  $\underline{B}$  required for currents parallel to  $\underline{B}$  above the Hall current region is small compared to errors in most measurements when the usual model computations for the parallel conductivity are used. Thus, existence of parallel currents does not imply strong parallel electric fields. Strong, i.e. about 20 volt/km, fields have however been reported by Mozer and Bruston (1967), Mozer and Fahleson (1970), and Kelley et al. (1971) from two rocket flights into the auroral belt ionosphere. These fields, deduced by testing for the magnitude of a parallel field that will reduce the rocket coning modulation of the component perpendicular to the rocket axis, are of long duration and spatial extent and thus are not to be confused with transient fluctuations. The validity of the technique depends on a number of factors which relate also to exact knowledge of vehicle trajectory and aspect, the instantaneous configuration of the wake of the vehicle and any appendages, and whether or not the effective contact potential of a probe changes when the ram direction shifts to various positions on the probe surface. Wake configurations are particularly critical when the coning angle is large and the probe separation is small. Kelley et al. (1971) conclude that the presence of anomalous resistivity, essential to support these strong fields, must also prevent  $Ba^+$  clouds from responding to parallel fields; inasmuch as large numbers (probably  $> 200$ )  $Ba^+$  clouds have been observed for extended periods of time without showing abnormal vertical motions. Theoretical analyses of  $Ba^+$  cloud motions, or dispersion, in the presence of anomalous resistivity have, however, not been made and evidence for the presence of anomalous resistivity has not been shown. Coincident changes in the perpendicular component measured by the probes, that would suggest corresponding polarization changes in  $\underline{E}$  perpendicular to  $\underline{B}$ , also appear to be lacking. In total, there are various grounds for skepticism regarding the validity of the parallel fields reported and there is an obvious need for 3-axis measurements with long baseline probes.

#### THE AURORAL BELT-POLAR CAP TRANSITION

As noted previously, poleward from the split in anti-solar convection at the Harang discontinuity and poleward from auroral latitudes on the dayside in the late morning hours, it is difficult to define an auroral belt-polar cap boundary, in terms of electric field directions, in that the anti-solar convection only gradually changes its direction. However, in the intervening local time sectors and particularly near the 18<sup>h</sup> and 6<sup>h</sup> meridians where the boundary involves a 180° field reversal, one can examine the form of the transition. Inasmuch as some magnetospheric models identify this boundary, or transition, in terms of a separation between open and closed field lines and/or the magnetopause, its sharpness is of some interest.

In Figure 1, for example, there are four boundary crossings: three of these appear as a gradual transition and one appears as a sharp step in the dawn-dusk component. This is rather typical although in general less than one in four would be as sharp as the one case in Figure 1. On the other hand the magnitude of a sudden change is sometimes greater and in these cases it might be appropriate to speak of a field shear at the boundary. In most cases, however, the boundary is best characterized as being either a gradual or irregular transition.

Several releases of multiple  $Ba^+$  clouds have been conducted in the boundary region. The releases shown in Figure 3 are perhaps unique in the sense that the clouds apparently circle the eye of a convective cell. In this case auroral arcs (not shown), aligned along invariant latitude lines, were located directly overhead at the POW-3 and BAR-M sites and to the south. The  $Ba^+$  clouds further south moved rapidly and uniformly westward as expected in the evening hours. For the high latitude releases, the initial motions of the first release (lowest latitude) and the final motions of the last release (highest latitude) were also westward. The second  $Ba^+$  cloud released from the high latitude site was apparently caught in the "eye" of the cell and moved very little during 33 minutes of observation. It is, of course, uncertain whether this is the "eye" of a cell covering a major fraction of the northern high latitudes or an "eddy" cell at the boundary. Convective continuity across the transition is, however, clearly apparent.

#### SPATIAL DISTRIBUTION OF POLAR CAP ELECTRIC FIELDS

The initial  $Ba^+$  releases within the polar cap (Wescott et al., 1970; Heppner et al. 1971) were conducted under  $K_p=3$  conditions and produced results that typify many subsequent measurements: i.e., "E was typically between 20 and 40 volts/km, directed roughly from dawn toward dusk, and was more uniform in space and time than  $E$  fields observed in the auroral belt." Subsequent polar cap  $Ba^+$  releases have purposely been conducted under a greater variety of conditions and a greater range of variability in magnitudes has been encountered. Injun-5 (Cauffman and Gurnett, 1971; Frank and Gurnett, 1971) and OGO-6 (Heppner, 1972a, c) (also see, reviews by Maynard, 1972; Cauffman, 1972) have provided a more comprehensive view of polar cap fields enabling one to examine its spatial distribution. Because of measurement thresholds Injun-5 results primarily relate to regions and times where the field exceeds 30 volts/km. It is evident in terms of the OGO-6 data, described below, that this places emphasis on occurrences of asymmetrical distributions.

Figure 1, particularly the top trace, illustrates a rather flat uniform polar cap field. This distribution occurs frequently but is only one of a number of different types of distributions that are found to recur at various times. The distribution along the two northern hemisphere traverses in Figure 4, in which the polar cap field intensity,  $|-E_x|$ , increases rather uniformly from evening towards morning illustrates another simple form of the distribution that frequently recurs. To determine how various distributions might relate to magnetic activity, interplanetary conditions, etc., Heppner (1972c) classified each dawn-dusk pass across the central part of the polar cap in terms of idealized "signatures" which represented the recurrent distributions. A larger fraction of the northern hemisphere passes could be unambiguously classified than for southern hemisphere passes: because, (a) the orbit and season placed a significant fraction of southern hemisphere passes near and in the region of high latitude dayside activity, and (b) the greater degree of irregularity in the southern hemisphere (Heppner, 1972a) made unambiguous signature identifications more difficult.

The importance of having both northern and southern hemisphere signature classifications is obvious from examples such as the successive passes over the two polar regions shown in Figure 4. In these passes the maximum,  $|E_x|$ , polar cap field intensity is on the morning side of the northern polar cap but on the evening side of the southern polar cap. This anti-correlation of asymmetrical distributions in the two hemispheres was apparent prior to use of the signature classifications noted above. The significance became apparent following correlation of signatures with interplanetary magnetic field directions, as discussed below.

For each pass across the northern or southern polar cap simultaneous values of the interplanetary magnetic field in solar-equatorial coordinates from the Ames magnetometer on Explorer-33 were recorded in terms of  $4^V$  buckets for the magnitude,  $B$ , eight angle sectors for the longitudinal angle,  $\phi$ , and six angle sectors for the latitudinal angle,  $\theta$ . Values were then grouped and plotted as histograms for each electric field signature in each hemisphere. In each case involving a signature for which there were many

passes (i.e., the most commonly occurring distributions) the  $\phi$  angle distribution was either concentrated in the two sectors between  $90^\circ$  and  $180^\circ$  (fields away from the sun) or concentrated in the two sectors between  $270^\circ$  and  $360^\circ$ . The interplanetary  $\theta$  angle (related to the north-south component of the interplanetary field), the field magnitude, B, and Kp values were found to be essentially uncorrelated with the type of electric field signature; however, relative to some signatures having features in common with others, shifts in the  $\theta$  angle histograms suggest that the  $\theta$  angle could possibly have some secondary influence on the  $\underline{E}$  field distribution.

For brevity, and illustration of the gross character of the  $\phi$  angle correlations, signatures involving the occurrence of a strong maximum on either the evening or morning side of the polar cap have been grouped in Figure 5. As indicated on the lower right of Figure 5, "flat" distributions across the northern polar cap have been grouped with cases of evening maximums in the northern polar cap. This is done because of similar  $\phi$  angle distributions and the fact that both of these contrast with cases of morning maximums in the northern polar region (upper right) and correlate relative to the  $\phi$  angle with morning maximums in the southern polar cap. 118 passes are represented: 34 from the southern hemisphere and 84 from the northern hemisphere (Note: southern hemisphere passes are from morning to evening, northern hemisphere passes are from evening to morning, and the sign of  $E_x$ , see Figures 1 and 4, is inverted in opposite hemispheres in spacecraft coordinates).

Figure 6, drawn for one orientation of the interplanetary magnetic field, suggests that the anti-correlation is a function of the relative orientation of the interplanetary magnetic field and the field direction in the outermost regions of the magnetosphere. That is, fast convection occurs on the side where the field lines are parallel and slow convection occurs on the side with anti-parallel field lines. This holds for both hemispheres and for the reverse direction of the interplanetary field. The implication appears clear; one needs to explain why the transfer of momentum (or convective velocity) from the solar wind is most effective in the case of parallel fields and least effective where the field lines are anti-parallel.

In Figure 7 asymmetrical distributions of the equipotentials (i.e., flow lines) are drawn to the right and left of an idealized symmetric distribution. In addition to the flow asymmetry, corresponding to the  $\phi$  angle shown and illustrated for the north polar cap, there is an additive asymmetric effect from boundary shifts accompanying the asymmetric flow. This comes from the observation that the polar cap-auroral belt boundary on the side where the flow is weak usually shifts toward the pole relative to its average position. To at least partially include this effect in Figure 7, the boundary has been shifted about  $3^\circ$  in latitude in the dawn-dusk direction, in an opposite sense in the left and right patterns. In many cases the shift is considerably greater as indicated in the examples of Figure 4. One consequence of both the asymmetric flow and the boundary shift is that the mid-day convection at auroral latitudes has continuity with either the morning auroral belt or evening auroral belt as a function of the  $\phi$  angle of the interplanetary field. The  $\phi$  angle has previously been found (Svalgaard, 1968; Mansurov, 1969) to correlate with the sign of  $\Delta Z$  at polar cap magnetic stations between  $83^\circ$  and  $88^\circ$  on the dayside near noon and the sign of  $\Delta H$  at slightly lower latitudes as indicated at the bottom of Figure 7. This is exactly the expected magnetic disturbance for ionospheric Hall currents accompanying the convection shown. The opposite, anti-correlated, distribution in the southern polar cap relative to a given  $\phi$  direction is also exactly what is required to obtain the proper signs for the simultaneous magnetic changes seen at southern polar cap magnetic observatories. Thus, the asymmetrical distributions of the polar cap electric fields and their dependence on interplanetary magnetic field directions, gives a physical explanation for the Svalgaard (1968) and Mansurov (1969) correlations.

#### MEASUREMENTS IN THE OUTER MAGNETOSPHERE

Initial efforts to directly measure d.c. electric fields in the outer magnetosphere and adjacent magnetosheath and interplanetary regions with a 20 meter baseline between double probes on OGO-5 demonstrated the necessity of using longer baselines in

regions where the ambient plasma flux is weak. D.C. measurements were, in general, valid only at and within the plasmapause. Much shorter baselines on Injun-5 (2.85 meters) (Cauffman and Gurnett, 1971) and S<sup>3</sup>-A (5 meters) (Maynard and Cauffman, 1972) have, respectively, shown limitations at altitudes near 2500 km in polar regions and well inside the plasmapause at the equator. A rather general condition has been that with short baselines very large signals can appear in response to decreases in the ambient plasma density and if not properly recognized as such, they could be incorrectly interpreted as d.c. field changes. This was particularly evident in magnetopause crossings of OGO-5.

Subsequently IMP-6 was launched with 3 pairs of long antenna probes with tip to tip lengths 7 meters axially and 52 and 92 meters in the spin plane giving baselines of 5.5, 35, and 75 meters, respectively. Roughly summarized for the outer regions of the magnetosphere: the shortest baseline (i.e., axial probes) has not given reliable measurements, the 35 meter baseline in select regions and for particular times has given reliable measurements but in general gives magnitudes which are too large and displaced in phase (relative to the longer baseline measurements), but, the 75 meter baseline appears to give valid measurements in most regions where E is greater than about 1 mv/meter. Weaker fields are frequently obscured by a variable sun-oriented sheath field but in some environments magnitudes as low as 0.3 mv/meter appear valid. Where the plasma flux is adequate, such that the values given by the 35 meter baseline decrease and approach the 75 meter baseline values, there is justification for confidence in the accuracy of the long baseline measurements. Confidence is also obtained from the agreement with  $\underline{v} \times \underline{B}$  for measured  $\underline{B}$  and typical  $\underline{v}$  values outside the magnetopause.

The preliminary results from these measurements (Aggson: personal communications) have been particularly significant in the vicinity of the magnetopause. Crossings analyzed are primarily near the equator in the 6 to 12<sup>h</sup> local time sector. First, exceptionally strong fields that would suggest a charge separation polarization have not been observed. Second, the convection,  $\underline{v}$ , observed adjacent to the magnetopause within the magnetosphere is consistently anti-solar, irregardless of the direction of the magnetosheath magnetic field (i.e.,  $\underline{E}$  reverses if  $\underline{B}$  reverses in crossing the boundary but does not reverse when the  $\underline{B}$  fields are parallel on opposite sides of the boundary). Third, the magnetospheric convection adjacent to the magnetopause is, as expected, generally slower than in the adjacent magnetosheath, but is fast compared to regions further from the boundary. In general this fast convection is limited to several minutes of time following a magnetopause crossing on inbound trajectories, but has been observed for as long as 20 minutes. Figure 8 illustrates a case where  $\underline{B}$  reversed on crossing the magnetopause and a corresponding 180° reversal of the  $\underline{E}$  field direction occurs, which means that the convective flow,  $\underline{v}$ , was parallel on opposite sides of the magnetopause. In this case the magnitude of  $\underline{E}$  (or  $\underline{v}$ ) was large for about 5 minutes following the crossing.

As the mapping of magnetic field lines from close to the magnetopause to the high latitude ionosphere cannot be accurately carried out in terms of existing magnetospheric models, it is not possible to state how and where the fast convection near the magnetopause fits into the high latitude measurements discussed earlier. This is a challenge for the future.

#### References

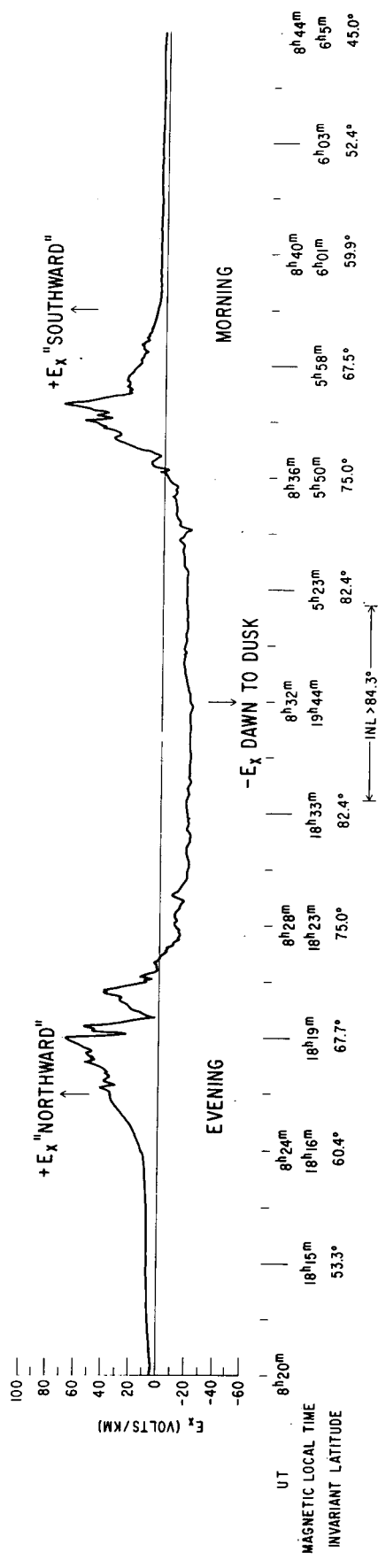
- Aggson, T. L. (1969): in Atmospheric Emissions (ed. by B. M. McCormac and A. Omholt) Van Nostrand Reinhold Co., New York, 305.
- Aggson, T. L. and Heppner, J. P. (1964) A proposal for electric field measurements on ATS-1, NASA-GSFC Report, July 1964.
- Aggson, T. L. and Bohse, J. R. (1972): AGU Annual Meeting (Abstract SM-73), 495.
- Axford, W. I. and Hines, C. O. (1961): Can. J. Phys., 39, 1433.
- Carpenter, D. L. and Stone, K. (1967): Planet. Space Sci., 15, 395.
- Cauffman, D. P. and Gurnett, D. A. (1971): J. Geophys. Res., 76, 6014.
- Cauffman, D. P. (1972: Space Sci. Rev. (to be published).

- Föpppl, H., Haerendel, G., Loidl, L., Lüst, R., Melzner, F., Meyer, B., Neuss, H., and Rieger, E. (1965). *Planet. Space Sci.*, 13, 95.
- Föpppl, H., Haerendel, G., Haser, L., Lüst, R., Melzner, F., Meyer, B., Neuss, N., Rabben, H., Rieger, E., Stocker, J., and Stoffregen, W. (1968). *J. Geophys. Res.*, 73, 21.
- Frank, L. A. and Gurnett, D. A. (1971). *J. Geophys. Res.*, 76, 6829.
- Haerendel, G., Lüst, R., Rieger, E., and Völk, H. (1969): in *Atmospheric Emissions* (ed. by B. M. McCormac and A. Omholt) Van Nostrand Reinhold Co., New York, 293.
- Haerendel, G. and Lüst, R. (1970): in *Particles and Fields in the Magnetosphere* (ed. by B. M. McCormac) D. Reidel Publ. Co., Dordrecht, 213.
- Haerendel, G. (1971): preprint of paper presented at the meeting "Earth's Particles and Fields," Cortina, Italy, Sept. 1971.
- Heppner, J. P. (1969): in *Atmospheric Emissions* (ed. by B. M. McCormac and A. Omholt) Van Nostrand Reinhold Co., New York, 251.
- Heppner, J. P., Stolarik, J. D., and Wescott, E. M. (1971): *J. Geophys. Res.*, 76, 6028.
- Heppner, J. P. (1972a): *Planet. Space Sci.*, 20 (in press).
- Heppner, J. P. (1972b): *Geophys. Publ.*, Special Edition, Minneskrift for Prof. L. Harang (ed. by J. Holtet and A. Egeland) (in press)
- Heppner, J. P. (1972c): presentation at AGU Annual Meeting, April 1972 (manuscript in preparation)
- Hines, C. O. (1964): *Space Sci., Rev.*, 3, 342.
- Kelley, M. C., Mozer, F. S., and Fahleson, U. V. (1971): *J. Geophys. Res.*, 76, 6054.
- Mansurov, S. M. (1969): *Geomag. and Aeron.*, 9, 622.
- Maynard, N. C. and Heppner, J. P. (1970): in *Particles and Fields in the Magnetosphere* (ed. by B. M. McCormac) D. Reidel Publ. Co., Dordrecht, 247.
- Maynard, N. C. (1972): *Proc. of the "Advanced Inst. on Magnetosphere-Ionosphere Interaction"*, Dalseter, Norway (to be published).
- Maynard, N. C. and Cauffman, D. P. (1972): presentation AGU Annual Meeting, April 1972 (manuscript in preparation).
- McIlwain, C. E. (1971): preprint of paper presented at the meeting "Earth's Particles and Fields," Cortina, Italy, Sept. 1971.
- Mozer, F. S. and Bruston, P. (1967): *J. Geophys. Res.*, 72, 1109.
- Mozer, F. S. and Serlin, R. (1969): *J. Geophys. Res.*, 74, 4739.
- Mozer, F. S. and Fahleson, U. V. (1970): *Planet. Space Sci.*, 18, 1563.
- Svalgaard, L. (1968): *Danish Meteor. Inst., Geophysical Papers*, R-6, August 1968.
- Wescott, E. M., Stolarik, J. D., and Heppner, J. P. (1969): *J. Geophys. Res.*, 74, 3469.
- Wescott, E. M., Stolarik, J. D., and Heppner, J. P. (1970): in *Particles and Fields in the Magnetosphere* (ed. by B. M. McCormac) D. Reidel Publ. Co., Dordrecht, 229.

## Figure Captions

- Figure 1: The horizontal component of the electric field perpendicular to the sun-earth line along two polar traverses of OGO-6 across the north magnetic pole.
- Figure 2: (a) typical motions of  $Ba^+$  clouds relative to the Harang discontinuity (solid arrows) and at locations remote from the Harang discontinuity (dotted arrows) from GSFC experiments (see text),  
(b) convective continuity near the Harang discontinuity,  
(c) ranges of variability in the location of the Harang discontinuity. Coordinates are magnetic time and invariant latitude.
- Figure 3: Tracks of four  $Ba^+$  clouds released simultaneously from each of two launch sites in Alaska during evening twilight. Four digit numbers along tracks are minutes and seconds.
- Figure 4: Highly asymmetric polar cap field distributions on successive passes of OGO-6 over the south and north magnetic poles. The sign of  $E_x$  is in spacecraft coordinates and is thus inverted in the two hemispheres. The arrow direction specifies the direction of increasing fields directed from dawn toward dusk (MLT = magnetic local time).
- Figure 5: (see text)
- Figure 6: (see text)
- Figure 7: (see text)
- Figure 8: IMP-6 electric field measurements along an inbound crossing of the magnetopause (dashed line) (from T. Aggson)

(Kp=3-) JUNE 11, 1969 E<sub>x</sub> = HORIZONTAL COMPONENT PERPENDICULAR TO SUN-EARTH LINE NORTHERN HIGH LATITUDES



(Kp=4-) JUNE 12, 1969 E<sub>x</sub> = HORIZONTAL COMPONENT PERPENDICULAR TO SUN-EARTH LINE NORTHERN HIGH LATITUDES

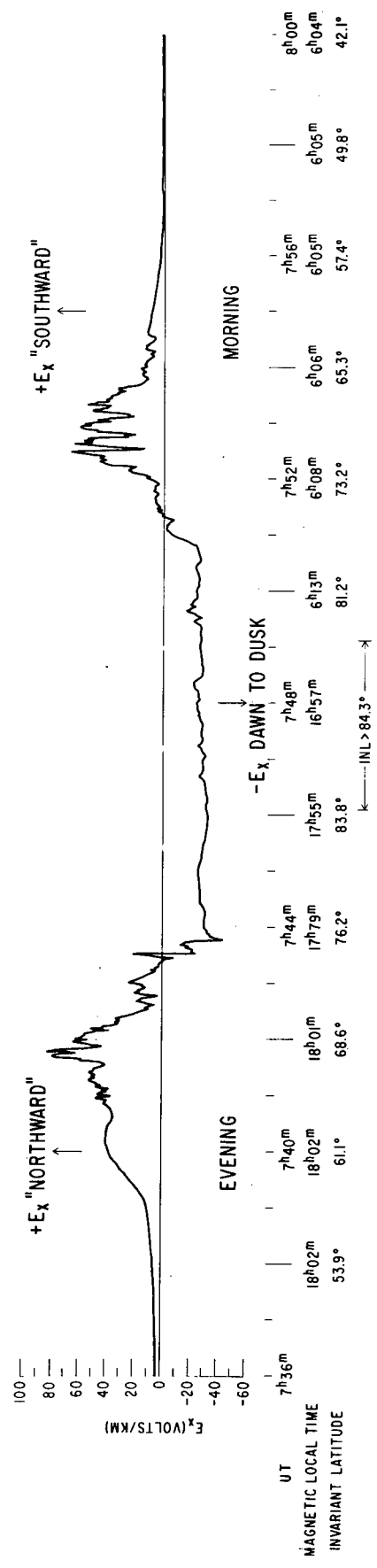


Figure 1

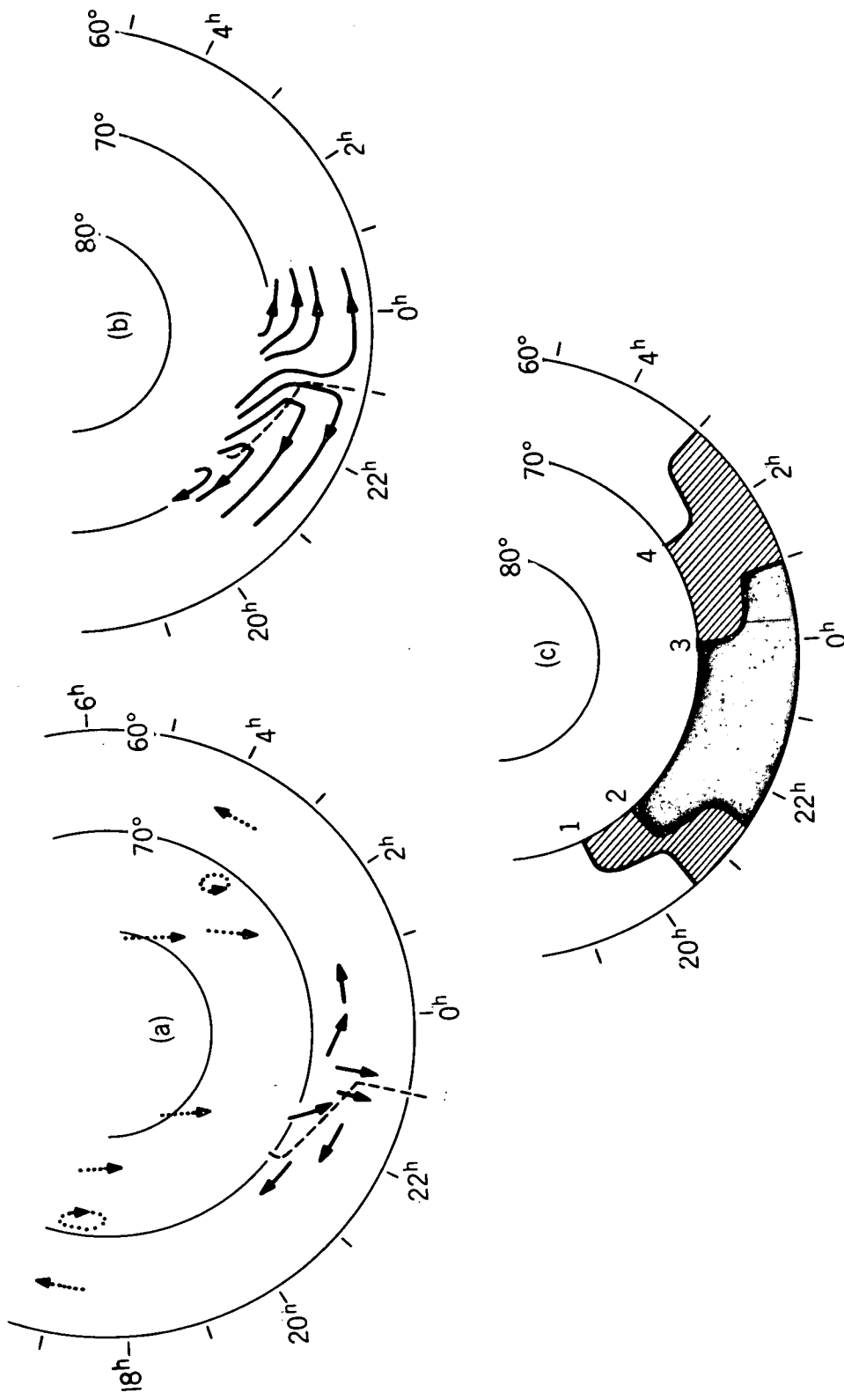


Figure 2

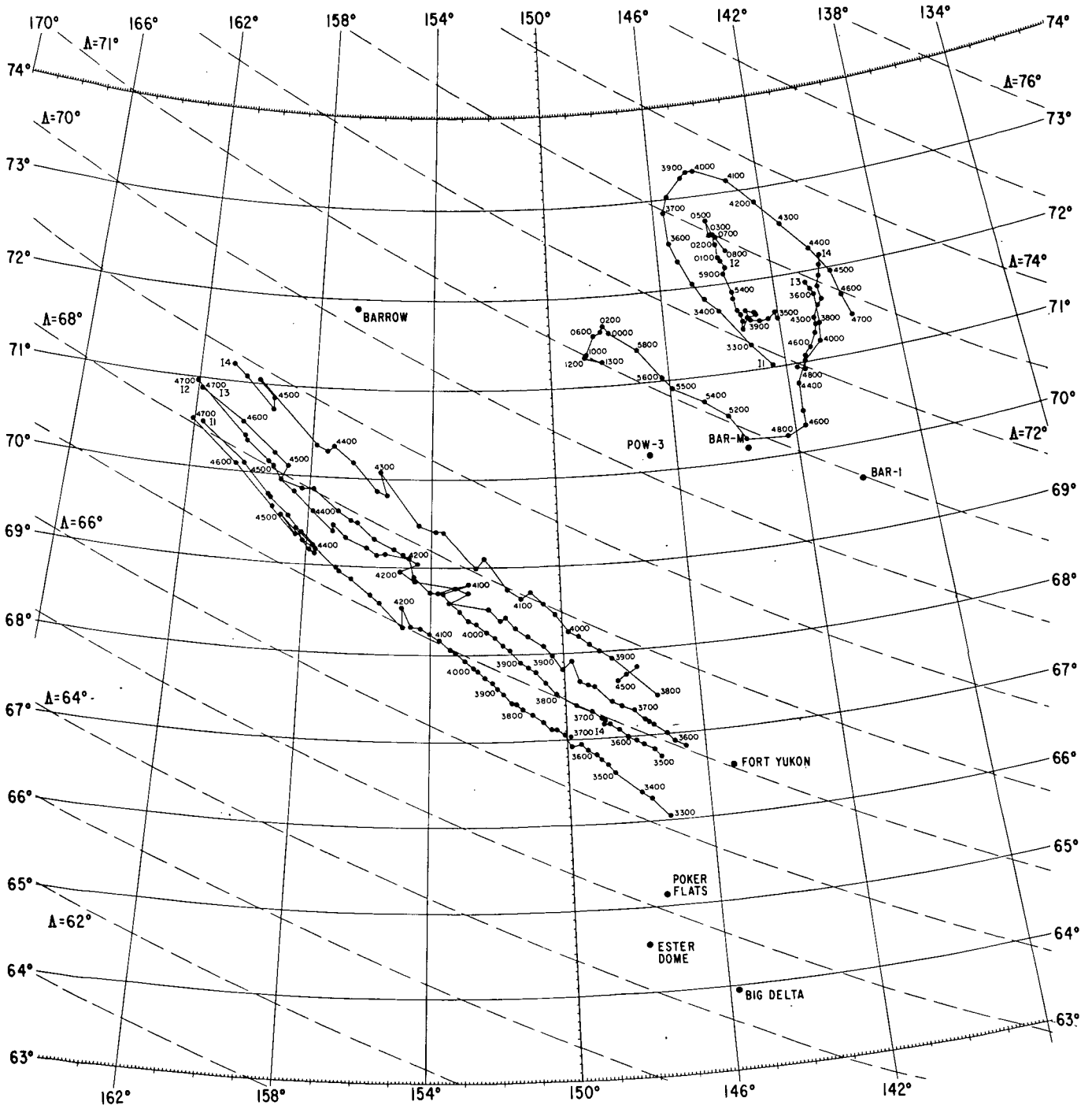


Figure 3

$E_x$  = HORIZONTAL COMPONENT PERPENDICULAR TO SUN-EARTH LINE

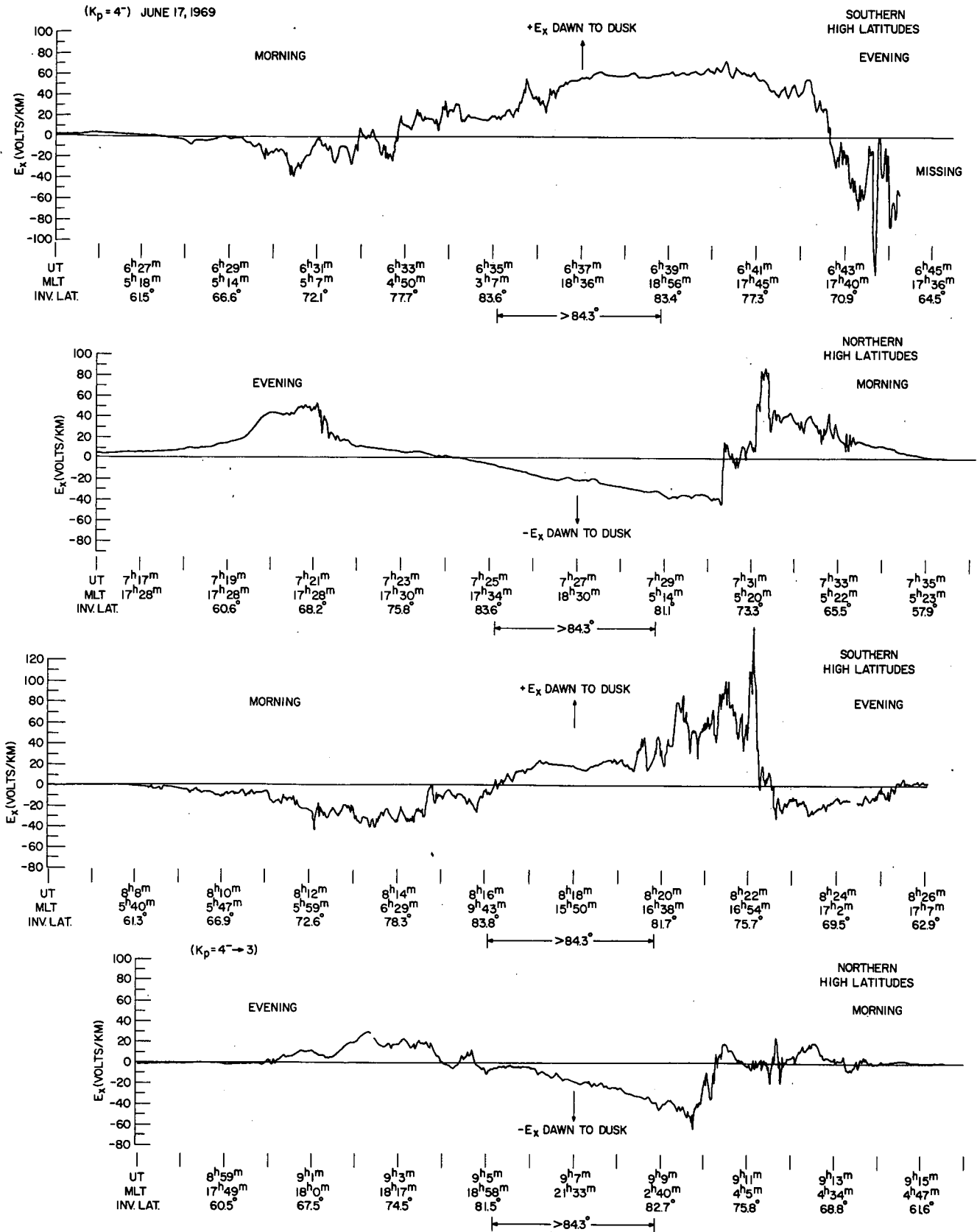


Figure 4

# ANTI-CORRELATED DISTRIBUTION OF THE DAWN-DUSK ELECTRIC FIELD ACROSS THE SOUTHERN AND NORTHERN POLAR CAPS

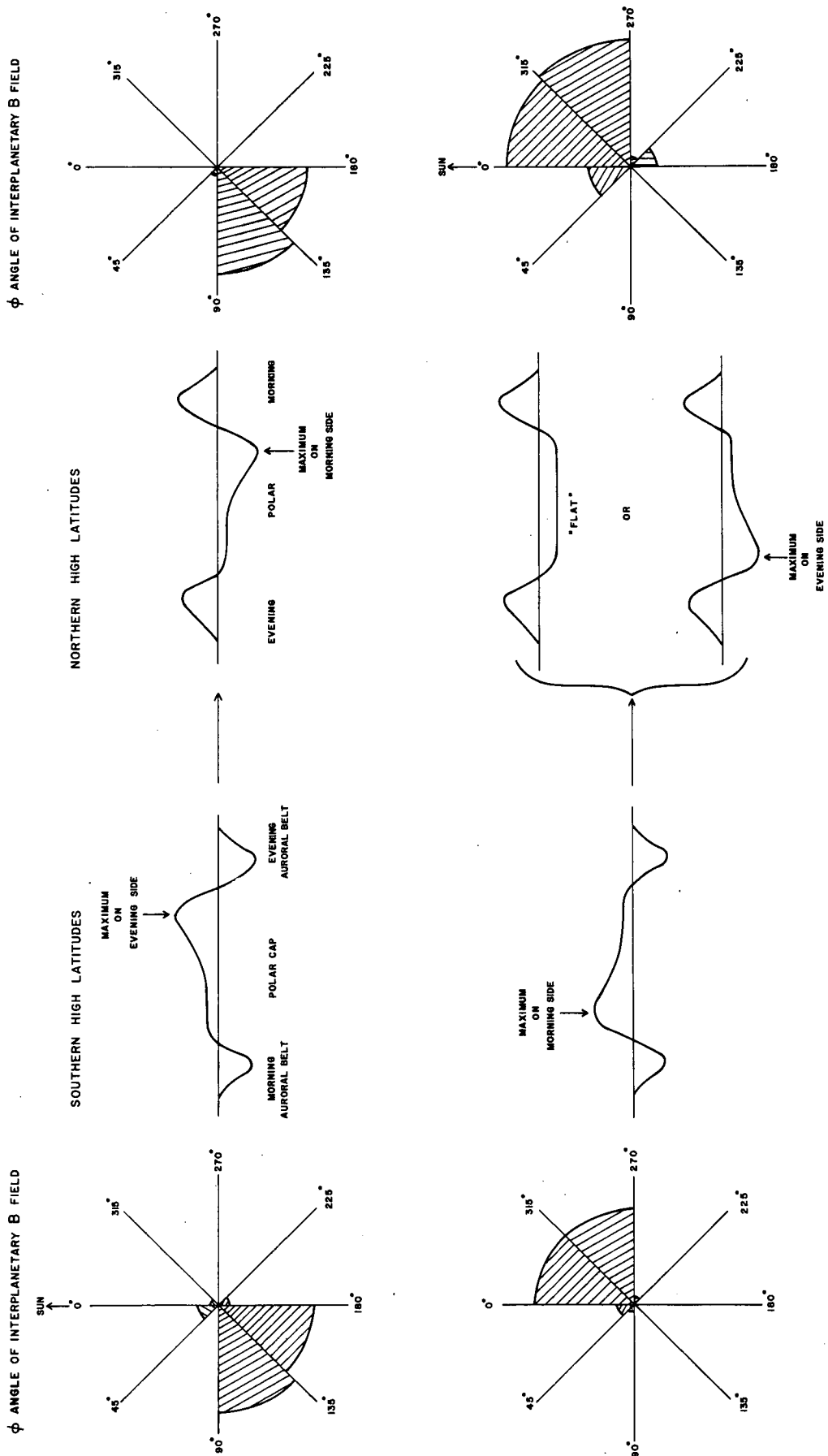


Figure 5

VIEW FROM ABOVE THE NORTH MAGNETIC POLE  
 ——— DISTORTED DIPOLE  $\vec{B}$  FIELD NEAR THE MAGNETOPAUSE ——— INTERPLANETARY  $\vec{B}$  FIELD

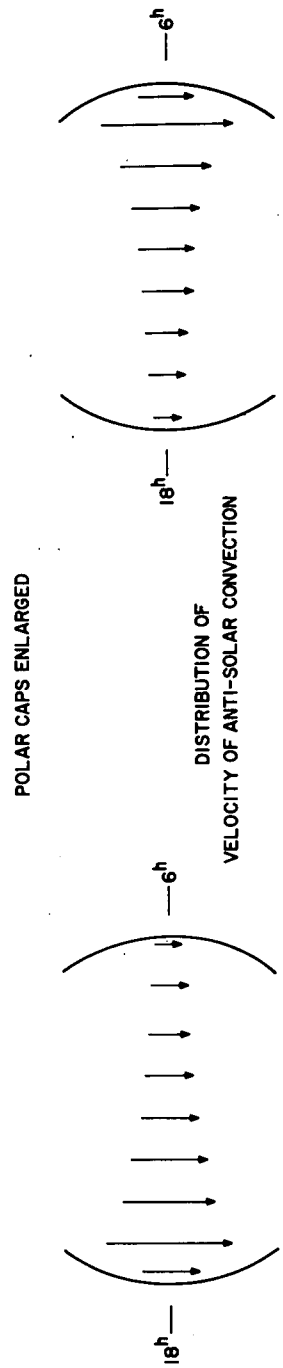


Figure 6

EXPLANATION OF CORRELATION BETWEEN  $\phi$  (or  $Y_{SE}$ ) AND DAYSIDE POLAR CAP  $\Delta Z$   
 FOUND BY SVALGAARD (1968), MANSUROV (1969), et al.

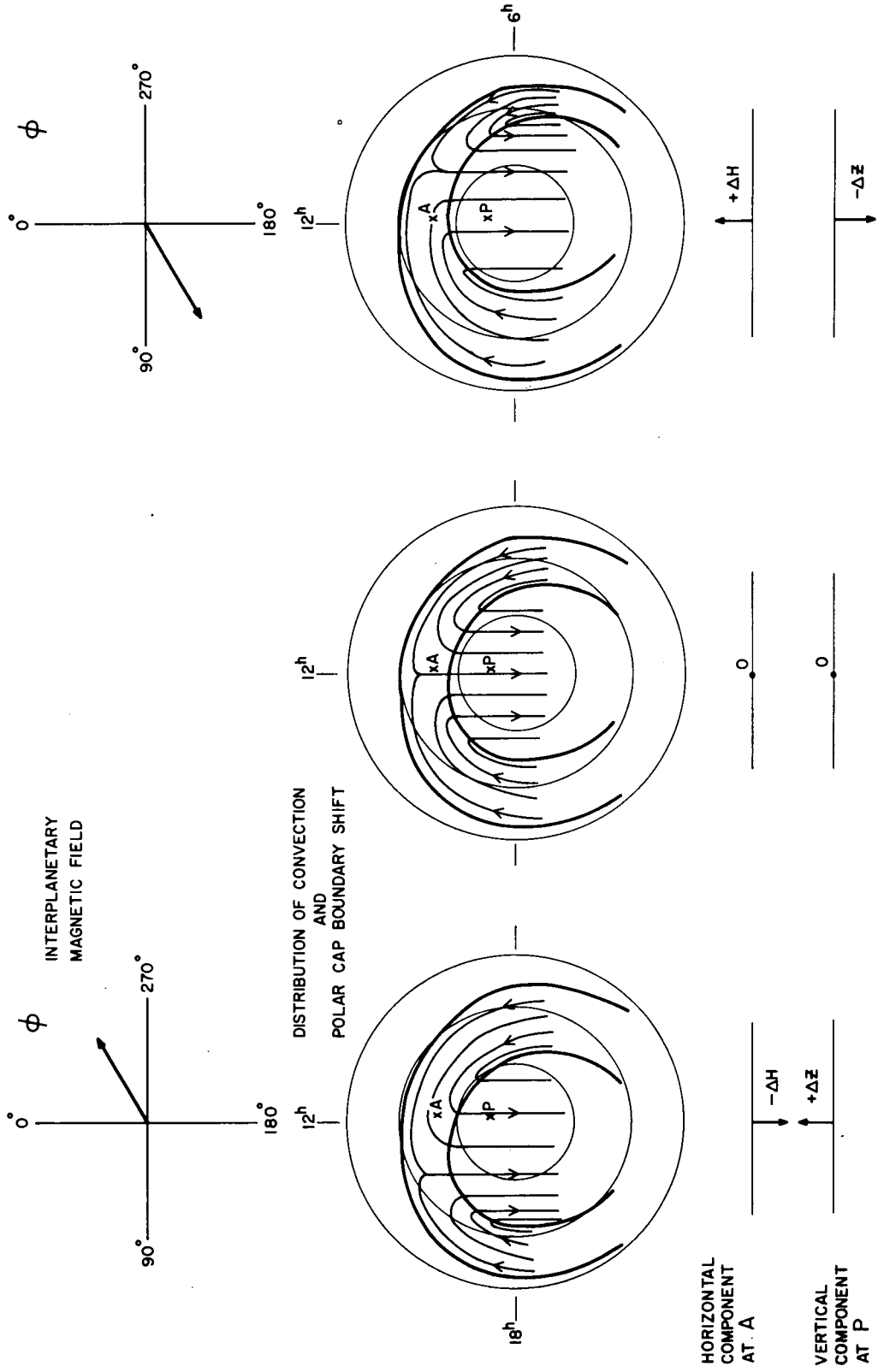
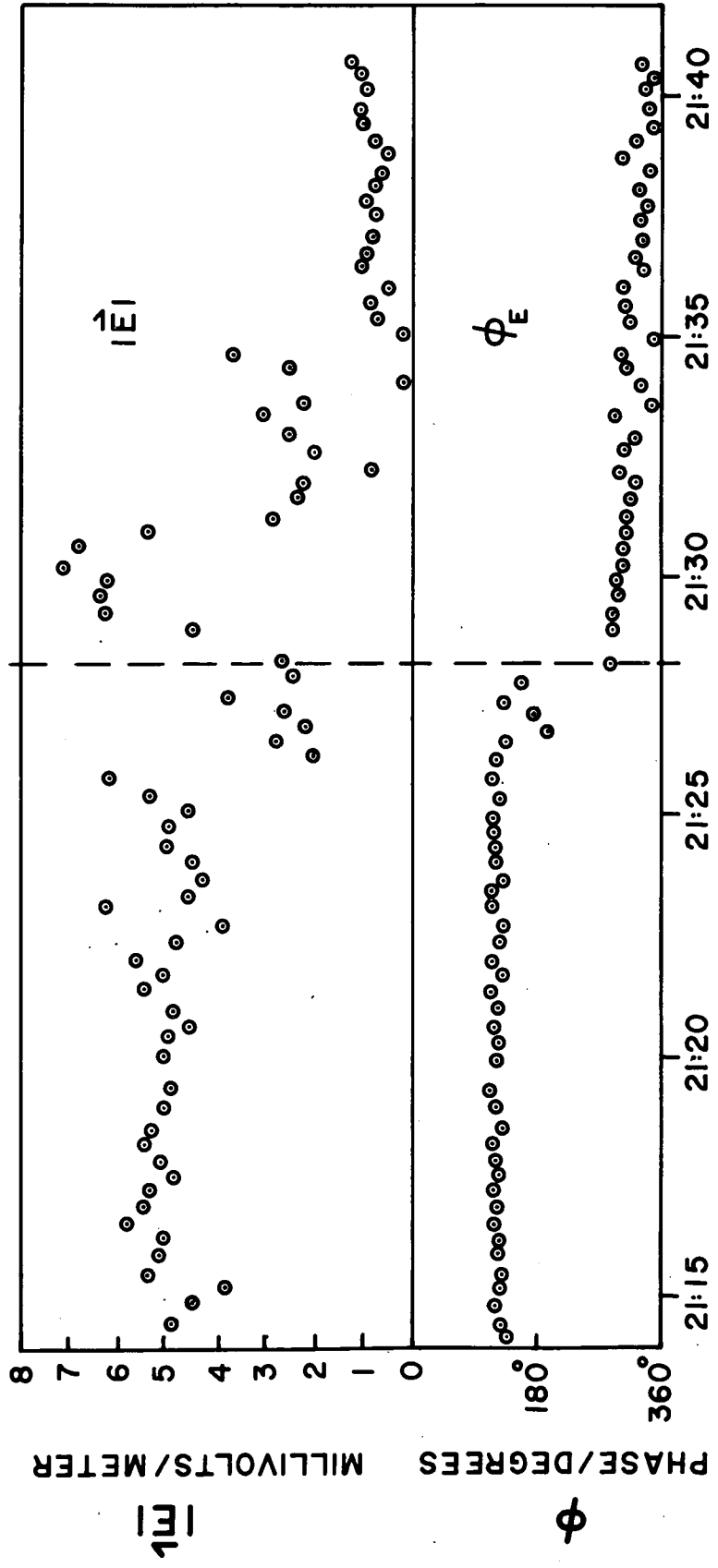


Figure 7

ORBIT 29  
MAGNETOPAUSE CROSSING  
INBOUND



TIME →

DAY 192, 1971  
IMP 6 DATA

Figure 8